Population Density Estimation for Dynamic Ground Risk Assessment of Drone Operations

Bizhao Pang
Air Traffic Management Research Institute, School of MAE
Nanyang Technological University
637460, Singapore
bizhao001@e.ntu.edu.sg

Xinting Hu
Air Traffic Management Research Institute, School of MAE
Nanyang Technological University
637460, Singapore
xinting002@e.ntu.edu.sg

Yi Yang Poh and Kin Huat Low
School of Mechanical and Aerospace Engineering
Nanyang Technological University
639798, Singapore
mkhlow@ntu.edu.sg

***Abstract*— Unmanned Aircraft Systems (UAS), also known as drones, have promising potential for integration into intelligent transportation systems to facilitate enhanced cargo and passenger flow. The escalating prevalence of UAS operations raises concerns regarding third-party ground risks, particularly within densely populated urban landscapes. Current mitigation strategies propose avoiding areas of high population density; however, these methodologies predominantly operate under the assumption that population density within specific locations remains static, which overlooks critical spatial-temporal population dynamics. This study introduces a prediction method with random forest regression to enhance the accuracy of population density estimations integral to risk assessment models. Obtained results were integrated into a gravity model to diffuse the predicted population volume at various time intervals, thereby generating dynamic risk maps. Finally, a graphic user interface is developed with backend computations to facilitate the decision makings for: 1) regulatory bodies to determine if a flight plan can be approved based on its risk cost and the target level of safety, and 2) UAS operators (e.g., drone delivery companies) to evaluate the overall risk level of their fleet by compute the risk cost of each flight plan. This work also contributes to the safety risk management of urban air mobility (UAM) in time-dependent ground risk mitigation.**

Keywords—Air traffic management, urban air mobility, third party risk, dynamic risk estimation, graphic user interface

I. INTRODUCTION

Unmanned aircraft system has been developing quickly with various applications in urban environments, such as cargo [1] and passenger transport [2] under the concepts of urban air mobility and advanced air mobility. It is envisioned as an intelligent, safe, and sustainable way of air transportation, which has the potential to reshape the urban transport system from two-dimension to three-dimension to enable better flows of cargo and passengers [3]. However, the predicted large-scale UAS operations in urban environments bring severe safety risk issues [4], as unmanned aircraft may crash and cause fatality risk to people on the ground. Ground fatality risk assessment and mitigation studies are therefore needed to improve the UAS operational safety.

Existing studies on ground fatality risk consider three key parameters, which are the probability of UAS system failure, the number of people hit by a crashed UAS, and the fatality rate of UAS accidents [5]. Among these parameters, the number of people hit by crashed UAS is a stochastic parameter, which is directly proportional to the population density. Most of the current studies assume that the population density in a specific area does not change over time [4], [6], [7], which is not practical as the spatial-temporal population movement is not captured by their models. To improve the accuracy of risk assessment results, temporal change in population density should be considered. Which requires the prediction of population density based on the historical population density distribution data.

To obtain the population density distribution, studies have been conducted by utilizing different sources of data. One group uses cell phone data [8], which gives the exact locations of population distribution at different timing. However, cell phone data is difficult to obtain, as it is highly restricted due to public privacy and security issues. Instead, the other group uses public transportation data (accounts for 70% of passengers) to capture the patterns of population movement within a city environment [9], which inspires the prediction of the spatial-temporal population movement in this research.

In this work, we have developed a population density prediction method to conduct the dynamic ground risk assessment. The method includes statistical analysis and a random forest regression model to process the passenger tape-in and tape-out data on a subway transportation system. With the model, we aim to improve the safety of UAS operations in urban areas by quantifying dynamic ground risk, to provide spatial-temporal risk information for time-dependent risk assessment and mitigation decisions.

II. RELATED WORKS

This section presents works on UAS risk assessment models and population density estimation methods.

A. UAS Risk Assessment Models

UAS may pose a risk to humans and vehicles on the ground when the pilot loses control or when it fails. Various methods can be used to reduce risk, including risk management, crash analysis, and UAS risk-based path planning with integrated risk cost [4]. Some risk management strategies include airspace [10], where UAS is allowed to operate in designated safe airspace. This is particularly effective in regions near airports where there is a high risk of collision with manned aircraft. Other methods for risk management include implementing rules and regulations for the authorization of UAS operations [5]. Crash or collision analysis can also be used to study, identify, and weigh the risk, which includes mathematical models for air traffic conflict and collision probability estimations [11].

Another branch of risk mitigation methods is risk-based path planning, where risk cost maps are generated [3], [12]. The risk cost maps help UAS operates safely by avoiding areas of high risk based on calculated third-party risk [6].

The risk maps can be split into static maps and dynamic ones [13]. Static risk mapping makes use of offline path planning to solve an optimal path planning problem with minimized risk cost. While dynamic risk mapping can be split into two types. Firstly, it can be used for online path planning to adjust the path based on real-time risk conditions observed during the flight. Secondly, dynamic risk mapping is done offline with predicted population density for time-dependent path planning. Other than using integrated 3D risk-based path planning, there are also studies on four-dimensional risk-based flight trajectory optimization [7], [14] with the objective of reducing ground fatality risk and airborne flight conflict risk.

The above-mentioned risk assessment and mapping studies focus on ground fatality risk, where population density is the critical factor. Prediction of population density helps to improving the accuracy of risk assessment for flight planning and risk management.

B. Population Estimation Used in Risk Assessment

The scope of this study focuses on the estimation of dynamic ground risk caused by spatial-temporal population density. To obtain the population density distribution, studies have been conducted by utilizing various sources of data, including personal cell phone data [15], remote sensing data [16], and public transportation data [17].

The benefit of using mobile phone data is the estimation accuracy, as the data tells the exact location and movement of people throughout the day [15]. However, the difficulty with this method is the availability of data. Mobile phone data sources are hard to come by due to privacy concerns. Another group utilizes the remote sensing data, which mainly includes population count data and land cover data from satellite imagery. The remote sensing data is always not overfitted, making the estimation results more accurate [16]. The disadvantage of this method, however, is that it requires many ancillary data sets that are expensive and difficult to process.

Existing methods look at the problem at the macro scale and try to predict and map out population density based on data. However, in urban areas, there are patterns of travel that can affect how populations are distributed throughout the day [18]. For instance, modelling the hourly distribution of the population at a high spatiotemporal resolution using subway smart card data has been tested [17], [19]. In these studies, the main patterns and trends of population movements were well captured, which inspires the application of using public transportation data to capture population density patterns.

III. Approach for Population Density Prediction

This section presents the detailed methodology of using historical public transportation data to predict the population density that is used for dynamic risk assessment. The census population density and mass rapid transit (MRT) data were obtained and employed in the training of a random forest regression model. The predicted population density was then diffused to areas without available data. The diffused population density was used in a ground risk assessment model to compute the time-dependent third-party risk.

The primary source to create the model for population density prediction is passenger volume by subway train station. This dataset provides the hourly tap-in and tap-out volumes for all MRT stations in Singapore, split into two types: weekdays and weekends. Geospatial data of the MRT locations are also obtained.

A. Data Preparation and Processing

Since public transportation system does not run 24 hours a day, there are missing values for time per hour. To help easier computation in later stages, time per hour values 0 and 1, which represent 0000hrs and 0100hrs are converted into 2400 and 2500hrs respectively. Another total volume is created to represent the summation of tap-in and tap-out volume. This value is used to estimate the population per hour of the MRT station. For each different type of area, two types of data from weekdays and weekends are analysed. The time per hour was set as the x-variable and the total volume as the y-variable.

After collating all the data from different months, the data is processed using Random Forest Regression (RFR) for each type of area. RFR method is a supervised learning algorithm that uses an ensemble learning approach for regression [20]. Multiple decision trees are ensembled to create a single model that is often more accurate compared to a single decision tree. RFR is the preferred method to find population density as the MRT tap-in and tap-out hourly data is non-linear and categorical. RFR is used in the work to determine the MRT usage for a specific period of a day. The data is split into 75% training and 25% testing. The mean squared error and R2 value of the training and testing data are compared with each other to evaluate the accuracy of the prediction at each dataset studied.

B. Population Density Diffusion with Gravity Model

After doing random forest regression, hourly prediction values for the population density in the MRT stations are obtained. To get finer dynamic population density values, based on intervals of five minutes, the hourly prediction is divided by 12. In this method, an assumption is made such that the number of people that tap-in and tap-out of the MRT in an hour is constant. With the prediction value of the MRT station at different periods, four different periods were selected, namely 0730, 1230, 1815, and 2200 to represent the population density patterns at morning peak, normal hours, evening peak, and night-time.

To obtain the predicted population density in areas where public transportation data is not available, a diffusion model is employed based on the concept of gravity model [21], which is presented as

$$\sigma_n = \sigma_{\mathrm{MRT}} e^{(1-r^2)} \tag{1}$$

$$r = \sqrt{(x_{\mathrm{MRT}} - x_n)^2 + (y_{\mathrm{MRT}} - y_n)^2} \tag{2}$$

where σ_n is the predicted population density of the n^{th} grid cell to the nearest MRT station, and σ_{MRT} is the predicted population density of the MRT station grid cell. Note that r is the Euclidean distance between the n^{th} grid cell and the grid cell of the MRT station. When r is less than 1 km, the gravity model applies. However, when r is greater than 1 km, the effects of the MRT dynamic population are diminished, and the static population of the area is used instead. Hence, when dynamic population density is applicable, the population density is calculated using the predicted population divided

by the area of the grid cell. When static population density is applicable, the census population of the subzone is used and divided by the area of the subzone.

C. Ground Risk Cost Assessment Model

UAS ground risk cost assessment model associated with population density is given in Equations (3) and (4). Here, P_{crash} is the probability of UAS system failure, N_{hit} is the number of pedestrians hit by a crashed UAS, and R_f is the fatality rate of UAS accidents. Note that σ_n is the predicted population density and S_{hit} is the size of the crash area.

$$C = P_{\text{crash}} N_{\text{hit}} R_f \tag{3}$$

$$N_{\text{hit}} = \sigma_n S_{\text{hit}} \tag{4}$$

Among these three factors, two of them, P_{crash} and R_f are constants, while N_{hit} is a quantifiable variable that is directly proportional to the population density, as obtained in Eq. (1). Since population density is directly proportional to UAS ground risk calculated from the diffusion process, the normalization of population density can explain UAS ground risk cost. Hence, normalized choropleth grid maps for UAS ground risk cost index are generated with a range of 0 to 1. The normalization is done by

$$c_{n,t} = \left(\frac{\sigma_{n,t} - \sigma_{\min}}{\sigma_{\max}} \right) w_t \tag{5}$$

where $c_{n,t}$ is the normalized risk cost index of the n^{th} grid cell at time t. Here, $\sigma_{n,t}$ is the predicted population density of the n^{th} grid cell at time t, and $\sigma_{\min}$ is the minimum predicted population density for the day, which also equals the static population density. Note that $\sigma_{\max}$ is the maximum predicted population density for the day, and w_t is the normalization factor at time t.

IV. Numerical Results and Discussions

In this section, we demonstrate: (1) the proposed methodology for dynamic population density prediction in various types of urban areas, (2) the predicted population density used in dynamic ground risk assessment and diffusions, and (3) the application of dynamic ground risk in a graphic user interface for UAS safety risk management.

A. Analysis for Population Density

Distinct types of areas have different dynamic population trends, as the purposes of population movement are different. For instance, the industrial area contains mostly offices and factories with little to no residents living in the area. The census population density is low, and most people only travel there for work purposes. Based on travel purposes, areas in urban environments can be classified into industrial, residential, central business districts, and commercial ones. Specific locations and census population density of each type used in this paper are shown in Table I.

TABLE I. AREAS OF STUDY.

Type	Location	Census Ppl. Den. (people/km^2)
Industrial area	Gul Circle	9
Residential area	Ang Mo Kio	60,266
Central business district	Raffles Place	316
Commercial area	Orchard	2,000

The historical population movement data for weekdays and weekends are obtained from 2022-07 to 2023-01, which are presented in **Fig. 1** and **Fig. 2**. From **Fig. 1**(a), it can be observed that the trend for the total tap-in and tap-out volumes of MRT is relatively constant between the months for weekdays at an industrial area. The data shows that MRT usage increases from 0500hrs to 0700hrs and from 1600hrs to 1700hrs then decreases from 0700hrs to 0900hrs and 1700 to 2000hrs. Distinct peaks at 0700hrs and 1700hrs can also be observed. A similar trend can be observed for the weekend population pattern as presented in **Fig. 2**(a). However, compared to weekday data, it is noted the overall usage is five times less during the peaks, from about 25000 on weekdays to about 5000 on weekends. This is because not

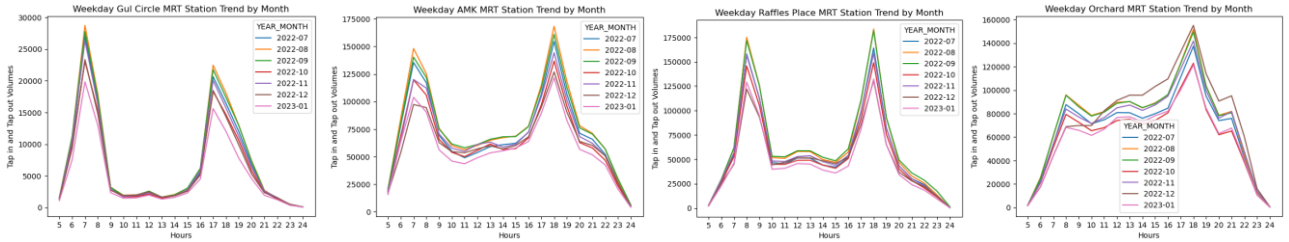

(a). Industrial (b). Residential (c). CBD (d). Commercial

Fig. 1. Weekday population density patterns at four different types of areas in urban environments.

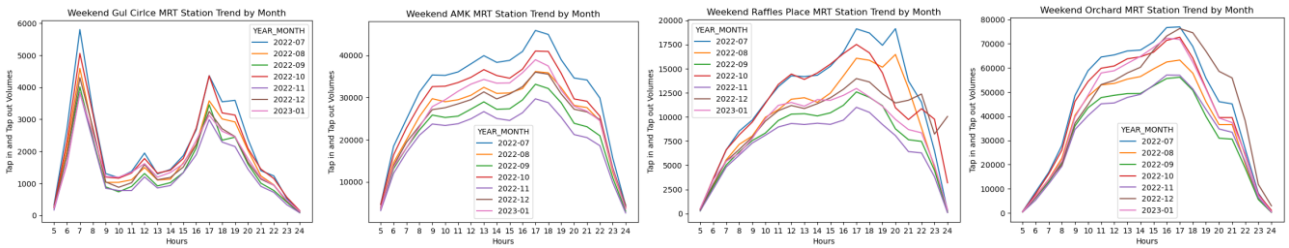

(a). Industrial (b). Residential (c). CBD (d). Commercial

Fig. 2. Weekend population density patterns at four different types of areas in urban environments.

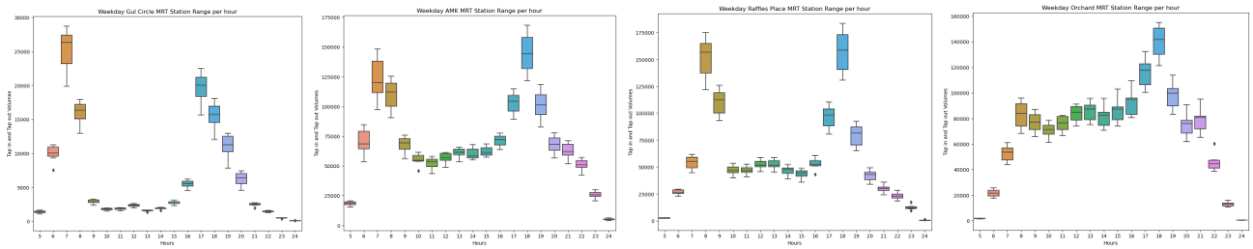

(a). Industrial (b). Residential (c). CBD (d). Commercial

Fig. 3. Weekday population density variance at four different types of areas in urban environments.

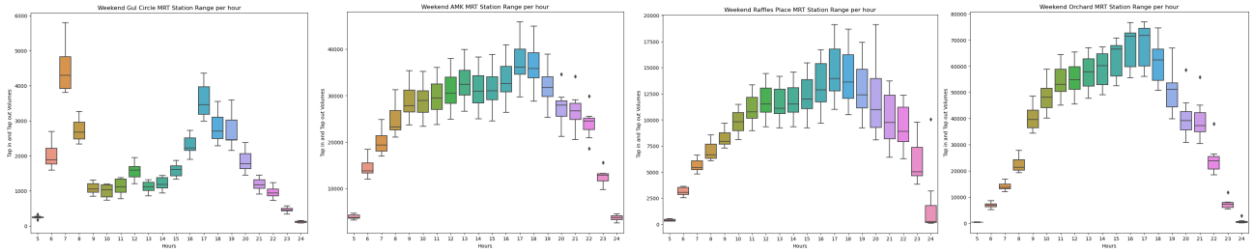

(a). Industrial (b). Residential (c). CBD (d). Commercial

Fig. 4. Weekend population density variance at four different types of areas in urban environments.

that many people travel to industrial areas for work on weekends.

Similar trends are also observed for residential areas (**Fig. 1**(b)) and CBD areas (**Fig. 1**(c)), where people travel from and to these two areas during morning and evening peak hours. A different population density pattern is shown in the commercial area (**Fig. 1**(d)) where the MRT usage sharply increases from 0500hrs to 0800hrs. Then the trend remains flat till 1600hrs. Then it increases and peaks at 1800hrs before it sharply decreases in the late evening hours.

On the other hand, different patterns are observed for weekend data against hours, compared with their weekdays' counterparts. The trend shows that population density increases sharply from 0500hrs to 0800hrs. Then it remains a slight increase trend throughout the afternoon. The peak density is at 1600hrs and 1700hrs. Then it decreases from 1800hrs to 2200hrs and sharply decreases at the late hours at night. It is noted that the general overall population density on weekends is three times less than on weekdays.

A notable observation from the data is that the variance is larger on weekend population density in each month, compared with weekday results, shown in **Fig. 3** and **Fig. 4**. That is because the commuting time and route for people on weekdays are more routine than on weekends, making the population movement patterns on weekday more regular with less variance among different months. The greatest variance of the population density is at morning and evening peak hours on weekdays, while in the afternoon and evening on weekends. Because commuters may not need to travel in the morning on weekends. The variances on weekends for the rest of the periods of the day are significantly larger than that of the weekday counterparts. A larger variance could affect the prediction performance. Detailed analysis for the prediction performance on population density is given below.

B. Prediction Performance on Population Density

In this subsection, the prediction is performed using random forest regression. The obtained prediction results for the four areas on weekdays and weekends are presented in **Fig. 5** and **Fig. 6** respectively. The average prediction performance on weekday population density is significantly better than weekend data (R^2_test_weekday = 0.909 vs. R^2_test_ weekend 0.794). That is because the commuting patterns of the population have fewer deviations during weekdays, as the time and route for commuting are more routine, compared with the weekend ones. For instance, the model performs well in the industrial area to a high degree of precision at all periods of the day as shown in **Fig. 5**(a), with R^2_train = 0.974, R^2_test = 0.967. However, the performance of the model is lower on weekends (R^2_train = 0.925, R^2_test = 0.901), shown in **Fig. 6**(a). Because there is a greater variance of trips generated on weekends, and it is difficult to explain the general purpose of people travelling to industrial areas on weekends.

For the results in residential area presented in **Fig. 5**(b), the model can predict the population density on weekdays in a densely populated residential area to a high degree of precision (R^2_test = 0.837) at most periods of the day. In the morning peak hours, the model over-predicts while in the evening, the model under-predicts. While the model generally underestimates the population density for weekend data, as shown in **Fig. 6**(b). Similar results are observed for CBD area (**Fig. 5**(c), and **Fig. 6**(c)) and commercial area (**Fig. 5**(d), and **Fig. 6**(d)), and the predicted population density is lower than actual ones in most of the periods. This could be a result of insufficient data used for the training of the prediction model.

An overall view of the prediction performance in different types of areas is given in **Fig.7**. The training performance of the model is better than the testing performance, especially for data from weekend residential and CBD areas. The reason could be the lack of sufficient data or more detailed feature selection, as in this work the hourly population density data is used for training and testing. A finer dataset can be used to further improve the prediction model in future works. While the performance on weekday results is notably better than that of the weekend

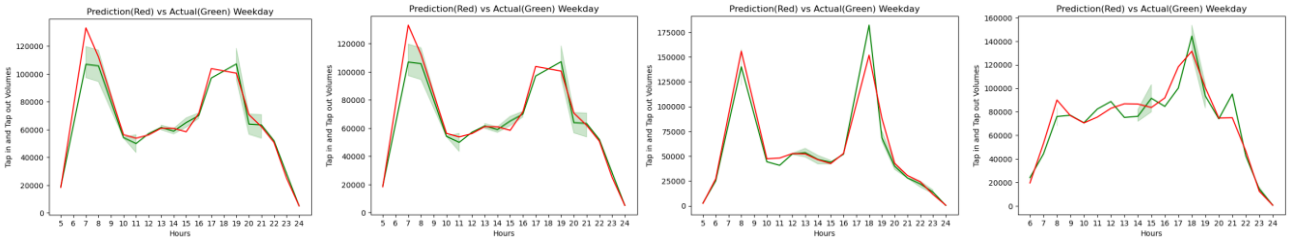

(a). Industrial (b). Residential (c). CBD (d). Commercial

Fig. 5. Prediction results of weekday data at four different types of areas in urban environments.

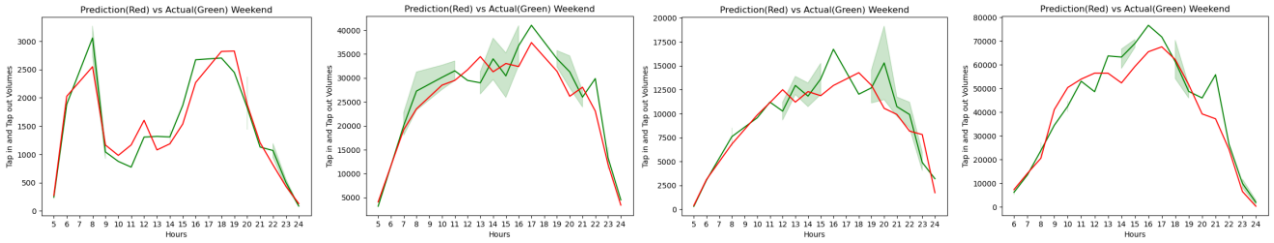

(a). Industrial (b). Residential (c). CBD (d). Commercial

Fig. 6. Prediction results of weekend data at four different types of areas in urban environments.

ones (R2_test_weekday =0.909 vs. R2_test_weekend 0.794). That is because the commuting patterns of the population have fewer deviations during weekdays, as the time and route for commuting are more routine, compared with the weekend ones.

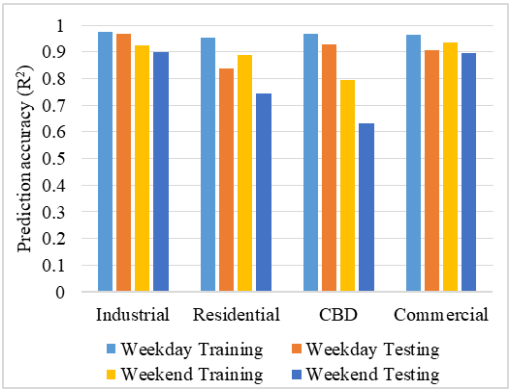

Fig.7. Comparison of prediction results on weekdays and weekends.

C. *Dynamic Risk Assessment Based on Predicted Results*

After obtaining the predicted population density, we compute dynamic ground risk for UAS operations. UAS risk cost index maps were generated at different timings, and an example is given with an industrial area (Gul Circle in Singapore) with weekend data to show changes in dynamic ground risk throughout the day. From **Fig. 8**, the drone risk index throughout the day can be observed for weekends on several key timings as defined in Section III. B. Drone risk at grid cells nearest to the MRT is significantly higher than those that are further due to diffusion of dynamic population density. At regions greater than one kilometre away from the MRT station, the population density is equivalent to census one. The risk cost index is the highest during the morning and evening peak hours, as the population densities are at their peaks during these periods.

D. *Graphic User Interface for Dynamic Risk Management*

We develop a graphic user interface (GUI) for dynamic risk management as shown in **Fig. 9**. The predicted population density is ingested into the risk assessment model to generate time-dependent risk cost, which is used to produce dynamic risk maps. By keying in the operation-related information such as UA type, expected take-off time, flight origin and destination, the risk cost of a flight path can be computed based on the predicted ground risk. That facilitates the decision makings for (1) civil aviation authorities to approve if the risk cost of a flight plan meets the target level of safety, and (2) UA operators (e.g., drone delivery companies) to evaluate the overall risk level of a fleet by compute the risk cost of each flight plan.

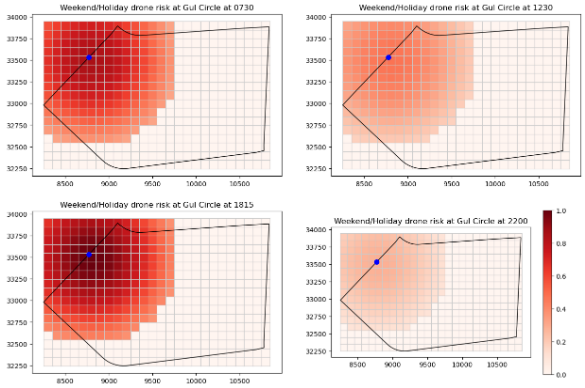

Fig. 8. Normalised ground risk at an industrial area.

V. CONCLUSIONS

This study proposes a methodology for dynamic ground risk assessment based on the prediction of population density. the prediction model employs the random forest regression method with the utilization of public transportation usage data. From the obtained prediction results, a diffusion method, predicated on the concept of the gravity model, has been established. This method diffuses the predicted volume across various time intervals, yielding dynamic population density values for each grid cell. Subsequently, risk cost index maps are generated based on the predicted population density, which could contribute to risk mitigation by identifying and avoiding high-risk areas depicted in the dynamic risk map.

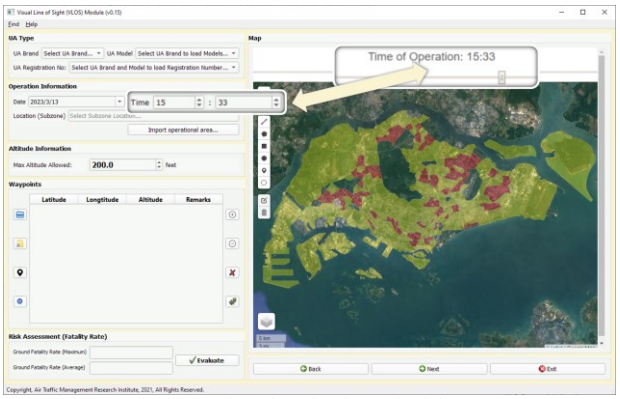

Fig. 9. Graphic user interface for dynamic risk management.

The study finds out that UAS ground risk associated with population density changes significantly throughout the day and a dynamic ground risk assessment method could improve risk mitigation for safe UAS operations. The prediction model performs well in areas where there is a predictable pattern of travel behaviour, such as places of industrial areas, where the trips generated for that location are relatively constant daily. It also performs well on weekdays, due to the predictable pattern of travel. However, the accuracy of the model is slightly compromised during weekends when temporal trends are less predictable due to uncertain travel behaviours.

The risk cost maps generated through this study can be integrated into risk-based path planning processes for more effective risk mitigation. The utility and effectiveness of these maps can be validated by contrasting them with existing risk cost path planning methodologies that use static population density as an input parameter. The results of this study stand to significantly enhance the safety of UAS operations by minimizing operational ground risks [22].

ACKNOWLEDGMENT

This research is supported by the National Research Foundation, Singapore, and the Civil Aviation Authority of Singapore, under the Aviation Transformation Programme. Any opinions, findings and conclusions or recommendations expressed in this material are those of the authors and do not reflect the views of National Research Foundation, Singapore, and the Civil Aviation Authority of Singapore.

REFERENCES

[1] M. Doole, J. Ellerbroek, and J. Hoekstra, “Estimation of traffic density from drone-based delivery in very low-level urban airspace,” J Air Transp Manag, vol. 88, Sep. 2020, doi: 10.1016/j.jairtraman.2020.101862.

[2] A. Straubinger, R. Rothfeld, M. Shamiyeh, K. D. Büchter, J. Kaiser, and K. O. Plötner, “An overview of current research and developments in urban air mobility – Setting the scene for UAM introduction,” J Air Transp Manag, vol. 87, no. June 2020, doi: 10.1016/j.jairtraman.2020.101852.

[3] B. Pang, W. Dai, T. Ra, and K. H. Low, “A Concept of Airspace Configuration and Operational Rules for UAS in Current Airspace,” in 2020 IEEE/AIAA 39th Digital Avionics Systems Conference (DASC), IEEE, 2020, pp. 1–9. doi: 10.1109/DASC50938.2020.9256627.

[4] B. Pang, X. Hu, W. Dai, and K. H. Low, “UAS path optimization with an integrated cost assessment model considering third-party risks in metropolitan environments,” Reliab Eng Syst Saf, vol. 222, no. February, p. 108399, 2022, doi: 10.1016/j.ress.2022.108399.

[5] JARUS, “JARUS guidelines on Specific Operations Risk Assessment (SORA), EDITION 2.0,” 2019. [Online]. Available: http://jarus-uas.org

[6] H. A. P. Blom, C. Jiang, W. B. A. Grimme, M. Mitici, and Y. S. Cheung, “Third party risk modelling of Unmanned Aircraft System operations, with application to parcel delivery service,” Reliab Eng Syst Saf, vol. 214, no. April, p. 107788, 2021, doi: 10.1016/j.ress.2021.107788.

[7] B. Pang, K. H. Low, and C. Lv, “Adaptive conflict resolution for multi-UAS 4D routes optimization using stochastic fractal search algorithm,” Transp Res Part C Emerg Technol, 2022, doi: 10.1016/j.trc.2022.103666.

[8] X. Yan, W. Wang, Z. Gao, and Y. Lai, “Universal model of individual and population mobility on diverse spatial scales,” Nat Commun, no. 8, pp. 1–9, 2017, doi: 10.1038/s41467-017-01892-8.

[9] Z. Cheng, M. Trépanier, and L. Sun, “Incorporating travel behavior regularity into passenger flow forecasting,” Transp Res Part C Emerg Technol, vol. 128, Jul. 2021, doi: 10.1016/j.trc.2021.103200.

[10] J. Cho and Y. Yoon, “How to assess the capacity of urban airspace: A topological approach using keep-in and keep-out geofence,” Transp Res Part C Emerg Technol, vol. 92, no. May, pp. 137–149, 2018, doi: 10.1016/j.trc.2018.05.001.

[11] M. Mitici and H. A. P. Blom, “Mathematical Models for Air Traffic Conflict and Collision Probability Estimation,” IEEE Trans. Intell. Transp. Syst., vol. 20, no. 3, pp. 1052–1068, 2019, doi: 10.1109/TITS.2018.2839344.

[12] B. Pang, Q. Tan, T. Ra, and K. H. Low, “A risk-based uas traffic network model for adaptive urban airspace management,” in AIAA Aviation 2020 Forum, pp. 1–9. doi: 10.2514/6.2020-2900.

[13] S. Primatesta, G. Guglieri, and A. Rizzo, “A Risk-Aware Path Planning Strategy for UASs in Urban Environments,” J. Intell. Robot. Syst.: Theory Appl., vol. 95, no. 2, pp. 629–643, 2019, doi: 10.1007/s10846-018-0924-3.

[14] W. Dai, B. Pang, and K. H. Low, “Conflict-free four-dimensional path planning for urban air mobility considering airspace occupancy,” Aerosp Sci Technol, vol. 119, p. 107154, 2021, doi: 10.1016/j.ast.2021.107154.

[15] P. Deville et al., “Dynamic population mapping using mobile phone data,” in Proc. Natl. Acad. Sci. U. S. A., 2014, pp. 15888–15893. doi: 10.1073/pnas.1408439111.

[16] A. E. Gaughan, F. R. Stevens, C. Linard, P. Jia, and A. J. Tatem, “High Resolution Population Distribution Maps for Southeast Asia in 2010 and 2015,” PLoS One, vol. 8, no. 2, Feb. 2013, doi: 10.1371/journal.pone.0055882.

[17] Y. Ma, W. Xu, X. Zhao, and Y. Li, “Modeling the hourly distribution of population at a high spatiotemporal resolution using subway smart card data: A case study in the central area of Beijing,” ISPRS Int J Geoinf, vol. 6, no. 5, May 2017, doi: 10.3390/ijgi6050128.

[18] J. Rappaport, “Consumption amenities and city population density,” Reg Sci Urban Econ, vol. 38, no. 6, pp. 533–552, 2008, doi: 10.1016/j.regsciurbeco.2008.02.001.

[19] A. K. Sivakumar, M. H. C. Man, and K. H. Low, “Spatiotemporal Population Movement for Ground Risk of Unmanned Aerial Vehicles (UASs) in Urbanized Environments using Public Transportation Data,” in AIAA Aviation 2022 Forum. doi: 10.2514/6.2022-3766.

[20] F. R. Stevens, A. E. Gaughan, C. Linard, and A. J. Tatem, “Disaggregating census data for population mapping using Random forests with remotely-sensed and ancillary data,” PLoS One, vol. 10, no. 2, Feb. 2015, doi: 10.1371/journal.pone.0107042.

[21] B. Pang, W. Dai, X. Hu, F. Dai, and K. H. Low, “Multiple air route crossing waypoints optimization via artificial potential field method,” Chin. J. Aeronaut., vol. 34, no. 4, 2021, doi: 10.1016/j.cja.2020.10.008.

[22] P. Gonçalves, J. Sobral, and L. A. Ferreira, “Unmanned aerial vehicle safety assessment modelling through petri Nets,” Reliab Eng Syst Saf, vol. 167, no. June, pp. 383–393, 2017, doi: 10.1016/j.ress.2017.06.021.